Understanding Simulations of Thin Accretion Disks by Energy Equation

Da-Bin Lin[1], Wei-Min Gu[1,2], Tong Liu[1], Mou-Yuan Sun[1], and Ju-Fu Lu[1]

ABSTRACT

We study the fluctuations of standard thin accretion disks by linear analysis of the time-dependent energy equation together with the vertical hydrostatic equilibrium and the equation of state. We show that some of the simulation results in Hirose et al. (2009b), such as the time delay, the relationship of power spectra, and the correlation between magnetic energy and radiation energy, can be well understood by our analytic results.

Subject headings: accretion, accretion disks - hydrodynamics - instabilities - MHD

1. Introduction

Aperiodic X-ray fluctuations have been observed from both galactic black hole binaries (BHBs) and active galactic nuclei (AGNs) (Uttley et al. 2005; McHardy et al. 2006). The Power Spectral Density (PSD) of such variability is generally modeled with a power law, $P(f) \propto f^{-\beta}$, where $P(f)$ is the power at frequency f, and β varies with frequency. In the soft state, the PSDs of both BHBs and AGNs have a steep slope with $\beta \sim 2$ at high frequencies, flatting to a shallow slope with $\beta \sim 1$ below a bend frequency $f_{\rm b}$, which is typically around 10Hz for BHBs (see King et al. 2004 and references therein). The PSDs in the hard state are more complex. The origin of variability is not well understood yet. However, it is highly tempting to relate this variability to the magnetohydrodynamic (MHD) turbulence, which is believed to drive the accretion process (Balbus & Hawley 1991). Some works followed this path through numerical simulation, and typically used proxies for the radiation rather than a direct measure of luminosity (Hawley & Krolik 2001; Noble & Krolik 2009). It remains uncertain whether the proxies for radiation are appropriate to describe the luminosity fluctuations. In the present work, we will show that the variability of magnetic

[1]Department of Physics and Institute of Theoretical Physics and Astrophysics, Xiamen University, Xiamen, Fujian 361005, China; dabinlin@xmu.edu.cn, lujf@xmu.edu.cn

[2]Harvard-Smithsonian Center for Astrophysics, 60 Garden Street, Cambridge, MA 02138, USA

energy (stress) of the standard thin disk is different from that of radiation for short time-scale fluctuations.

Recently, shearing box simulations of stratified magnetorotational turbulence (Hirose et al. 2009b) showed that fluctuations in the magnetic energy (stress) lead those in the radiation energy with roughly a thermal time-scale, and a correlation is found between the stress and total pressure. Moreover, the disk is found to be thermally stable, which is, however, in conflict with the disk theory (Lightman & Eardley 1974; Shakura & Sunyaev 1973). The discrepancy reveals that the correlation found in the simulation may be different from the α-prescription. For example, such a correlation may be related to the energy equation or result from the feedback from pressure to stress, which is not in the form of the standard α-prescription (e.g., Lin et al. 2011; Ciesielski et al. 2012). Since the dissipation of magnetic energy will heat the gas of accretion flow, the perturbations in the magnetic energy will produce corresponding fluctuations in the internal energy and therefore in the pressure. Then, there should exist a correlation and delay between the stress and the pressure. In the present work, based on the energy equation, we will investigate the relationship between fluctuations of the viscous heating and the inducing fluctuations of the radiative cooling.

The paper is organized as follows. The relationship of fluctuations of the viscous heating and the inducing fluctuations of the radiative cooling is derived in Section 2. A comparison of analysis and simulation is presented in Section 3. Conclusions and discussion are made in Section 4.

2. Radiative cooling fluctuations induced by viscous heating fluctuations

2.1. Energy equation

In the context of standard thin accretion disk (Shakura & Sunyaev 1973), the vertically integrated energy equation in cylindrical coordinates (r, ϕ, z) takes the form (e.g., Kato et al. 2008):

$$\frac{\partial E}{\partial t} - (E + \Pi)\frac{\partial \ln \Sigma}{\partial t} + \Pi \frac{\partial \ln H}{\partial t} = Q^{+}_{\rm vis} - Q^{-}_{\rm rad} \ , \tag{1}$$

where H is the vertical height of the disk, and $\Sigma\,(= 2\rho H)$ and $\Pi(= 2pH)$ are the surface density and the vertically integrated pressure, respectively. The gas internal energy E and the radiative cooling rate $Q^{-}_{\rm rad}$ per unit area are expressed as

$$E = E_{\rm rad} + E_{\rm gas} = \left[3(1-\beta) + \frac{\beta}{\gamma - 1}\right]\Pi \ , \tag{2}$$

$$Q^{-}_{\rm rad} = \frac{16acT^4}{3\bar{\kappa}\Sigma} \ , \tag{3}$$

where $E_{\rm rad}$ and $E_{\rm gas}$ are respectively the internal energy of radiation and gas, β is defined as the ratio of the gas to the total pressure, i.e., $\beta \equiv \Pi_{\rm gas}/\Pi$, γ is the ratio of specific heating, and T is the temperature on the equatorial plane of the disk. The opacity $\bar{\kappa}$ is generally dominated by the electron scattering ($\kappa_{\rm es}$) in radiation-pressure-dominated accretion disks, where $\bar{\kappa}$ can be regarded as a constant. On the other hand, if the opacity is dominated by the free-free absorption ($\kappa_{\rm ff}$), $\bar{\kappa}$ will vary with the temperature and the density. The viscous heating $Q^{+}_{\rm vis}$ is due to the dissipation of magnetic energy and turbulent kinetic energy in magnetoturbulent disks, and is dominated by the dissipation of magnetic energy in simulations (Simon et al. 2009).

For the fluctuations with a time-scale less than the viscous time-scale, the variation of Σ can be neglected, and Equation (1) is therefore simplified as

$$\frac{\partial E}{\partial t} + \Pi \frac{\partial {\rm ln} H}{\partial t} = Q^{+}_{\rm vis} - Q^{-}_{\rm rad}. \tag{4}$$

In order to study the induced fluctuations of radiative cooling, we adopt the vertical hydrostatic equilibrium

$$\Omega^2_{\rm K} H^2 = \frac{\Pi}{\Sigma}, \tag{5}$$

and the equation of state, which can be approximately expressed as

$$\Pi = \Pi_{\rm gas} + \Pi_{\rm rad} = \frac{k_{\rm B}}{\mu m_{\rm H}} \Sigma T + \frac{2}{3} a T^4 H. \tag{6}$$

2.2. Relationship of fluctuations

We use the subscripts "0" and "1" to describe the unperturbed and perturbed quantities, respectively. We would stress that, the amplitude of fluctuations is assumed to be small in our linear analysis. In simulations (e.g., Figures 3 and 4 of Hirose et al. 2009b), however, the amplitudes can be significantly large. Nevertheless, the linear analysis may reveal the relationship of fluctuations of physical quantities. Combining Equations (2)-(6) with $\bar{\kappa} = \kappa_{\rm es}$, we have

$$A t_{\rm th} \frac{\partial}{\partial t} (4 \frac{T_1}{T_0}) = \frac{Q^{+}_{\rm vis,1}}{Q^{+}_{\rm vis,0}} - 4 \frac{T_1}{T_0}, \tag{7}$$

where the dimensionless parameter A is expressed as

$$A = \frac{(4-3\beta)(\gamma-1)}{4(1+\beta)\left[\beta + 3\left(1-\beta\right)\left(\gamma-1\right)\right]} \left[7 - 6\beta + \frac{2\beta}{\gamma-1} - \frac{7\beta\left(4-3\gamma\right)\left(1-\beta\right)}{\left(\gamma-1\right)\left(4-3\beta\right)} \right], \tag{8}$$

and the thermal time-scale $t_{\rm th}$ takes the from (with $Q^+_{\rm vis,0} = 3\alpha\Pi_0\Omega_{\rm K}/2$):

$$t_{\rm th} \equiv \frac{E_0}{Q^-_{\rm rad,0}} = \frac{E_0}{Q^+_{\rm vis,0}} = \left[2\left(1-\beta\right) + \frac{2\beta}{3(\gamma-1)}\right]\frac{1}{\alpha\Omega_{\rm K}}. \tag{9}$$

We choose $\gamma = 5/3$ and $\alpha = 0.02$ (e.g., Hirose et al. 2009a) for numerical calculations. The variation of A with β is shown by the solid line in Figure 1. The other two parameters, $A_{\rm ff}$ (dashed line) and $A_{\rm rad}$ (dotted line), will be introduced by Equations (13) and (16), respectively.

By assuming that the time-dependent component of fluctuations takes the form of $\exp(i\omega t)$, e.g., $Q^+_{\rm vis,1}/Q^+_{\rm vis,0} \propto \exp(i\omega t)$, we have the following relationship from Equation (7):

$$\left(4\frac{T_1}{T_0}\right)_\omega = \frac{1}{iA\omega t_{\rm th}+1}\left(\frac{Q^+_{\rm vis,1}}{Q^+_{\rm vis,0}}\right)_\omega, \tag{10}$$

where $\left(Q^+_{\rm vis,1}/Q^+_{\rm vis,0}\right)_\omega$ and $\left(4T_1/T_0\right)_\omega$ represent the fluctuations with ω of the viscous heating and those of the radiative cooling, respectively. We would stress that Equation (10) is a key relationship in the present work.

3. Comparison of analysis and simulation

3.1. Time delay between magnetic energy and radiation energy

Equation (10) can be modified as

$$\left(4\frac{T_1}{T_0}\right)_\omega = \frac{1}{\sqrt{\left(A\omega t_{\rm th}\right)^2+1}}\left(\frac{Q^+_{\rm vis,1}}{Q^+_{\rm vis,0}}\right)_\omega \exp\left(-i\omega t_{\rm del}\right), \tag{11}$$

where the delay time $t_{\rm del}$ of the radiative cooling compared with the viscous heating takes the form:

$$t_{\rm del} = \frac{1}{\omega}\arctan\left(A\omega t_{\rm th}\right). \tag{12}$$

Obviously, this equation implies $t_{\rm del} \approx A t_{\rm th}$ for long time-scale fluctuations.

Figure 2 shows the variation of $t_{\rm del}$ for three different values of β. The simulations for $\beta \sim 0.1$ (Hirose et al. 2009b) showed that fluctuations of magnetic energy lead those of radiation energy by $5-15$ orbit periods ($t_{\rm orb}$), roughly a thermal time. Moreover, Figure 5 of Hirose et al. (2009b) indicates that significant variability occurs in the range $0.01 \lesssim f\cdot t_{\rm orb} \lesssim 0.1$, which is equivalent to $0.01 \lesssim \omega/\Omega_{\rm K} \lesssim 0.1$, corresponding to the region between the two

vertical dot-dashed lines in Figure 2. As shown by the solid line, the delay in our analysis is around $3-17t_{\rm orb}$, which is consistent with the simulations. In addition, we would point out that the delay between viscous heating and magnetic energy ($\sim 0.5t_{\rm orb}$, Hirose et al. 2009b) is negligible compared with the thermal time-scale.

Furthermore, simulations have been done for the gas-pressure-dominated case (Hirose et al. 2006) and the case that gas and radiation pressures are comparable (Krolik et al. 2007). The delay in those simulations is $\sim 2t_{\rm orb}$ for $\beta \sim 0.8$ and $\sim 5t_{\rm orb}$ for $\beta \sim 0.5$. In our analysis, as shown by the dotted and dashed lines, the delay is around $2-3t_{\rm orb}$ for $\beta = 0.8$ and $2-12t_{\rm orb}$ for $\beta = 0.5$ in the range $0.01 \lesssim \omega/\Omega_{\rm K} \lesssim 0.1$, which is again consistent with the simulations. Note that $\bar{\kappa}$ in the simulations for $\beta \sim 0.8$ (Hirose et al. 2006) is dominated by the free-free absorption. In such case, for a simple approach, we modify the parameter A as $A_{\rm ff}$ by considering the free-free absorption instead of the electron scattering in Equation (3):

$$A_{\rm ff} = \frac{(4-3\beta)(\gamma-1)}{(11.5+4.5\beta)\left[\beta+3\left(1-\beta\right)\left(\gamma-1\right)\right]}\left[7-6\beta+\frac{2\beta}{\gamma-1}-\frac{7\beta\left(4-3\gamma\right)\left(1-\beta\right)}{\left(\gamma-1\right)\left(4-3\beta\right)}\right]. \quad (13)$$

The profile of $A_{\rm ff}$ is shown by the dashed line in Figure 1.

3.2. Power spectrum relationship

In this subsection, we will show a comparison between our analytic normalized power spectrum of radiation energy $P^{\rm A}_{\rm rad}$ and that in simulations $P_{\rm rad}$. Equation (11) provides the relationship of the power spectrum between the radiative cooling $P_{\rm cool}$ and the viscous heating $P_{\rm vis}$:

$$P_{\rm cool}(f) = \frac{1}{1+(2\pi A f t_{\rm th})^2} P_{\rm vis}(f). \quad (14)$$

Then the analytic power spectrum of volume-integrated radiation energy $P^{\rm A}_{\rm rad}$ is expressed as

$$P^{\rm A}_{\rm rad}(f) = \frac{A^2_{\rm rad}}{1+(2\pi A f t_{\rm th})^2} P_{\rm vis}(f), \quad (15)$$

where the quantity $A_{\rm rad}$ is derived from Equations (2), (5), and (6):

$$A_{\rm rad} \equiv \frac{(E_{\rm rad,1}/E_{\rm rad,0})}{(4T_1/T_0)} = 1+\frac{4-3\beta}{4(1+\beta)}. \quad (16)$$

The variation of $A_{\rm rad}$ with β is shown by the dotted line in Figure 1. Since the viscous heating is mainly due to the dissipation of magnetic energy, it is plausible to have

$$P_{\rm vis}(f) \approx \left[(\sqrt{2}\pi f t_{\rm dis})^2+1\right] P_B(f), \quad (17)$$

where $t_{\rm dis}$ is the dissipation time-scale of magnetic energy, and P_B is the power spectrum of magnetic energy. The explanation for this relationship is presented in Appendix A. Then, Equations (15) and (17) provide an analytic relationship between the power spectrum of radiation energy and that of magnetic energy:

$$P_{\rm rad}^{\rm A}(f) = A_{\rm rad}^2 \frac{1+\left(\sqrt{2}\pi f t_{\rm dis}\right)^2}{1+\left(2\pi A f t_{\rm th}\right)^2} P_B(f). \tag{18}$$

The simulations (Equation (17) and Figure 5 of Hirose et al. 2009b) showed the profiles of P_B and $P_{\rm rad}$:

$$P_B\left(f\right) = \begin{cases} 8.7\times10^{-6} f^{-1.13}, & f < 0.171, \\ 10^{-7} f^{-3.65}, & f > 0.171, \end{cases} \tag{19}$$

$$P_{\rm rad}\left(f\right) = \begin{cases} 6.1\times10^{-9} f^{-2.38}, & f < 0.118, \\ 2.3\times10^{-10} f^{-3.91}, & f > 0.118. \end{cases} \tag{20}$$

In our Figure 3, we replot the above P_B and $P_{\rm rad}$ with the dotted and dashed lines, respectively. In addition, according to Equation (18), we plot the analytic power spectrum $P_{\rm rad}^{\rm A}$ with the solid line. The values of $P_B(f)$ in Equation (18) are taken from the above simulation results (the dotted line). The parameters for calculating $P_{\rm rad}^{\rm A}$ are $A = 2.1$, $A_{\rm rad} = 1.8$ (corresponding to $\beta = 0.1$), and $t_{\rm dis} = 0.5 t_{\rm orb}$ (Hirose et al. 2009b). As shown by the solid and dashed lines, our analytic $P_{\rm rad}^{\rm A}$ agrees well with $P_{\rm rad}$ in simulations.

3.3. Correlation between magnetic energy and radiation energy

The energy equation implies a correlation between the viscous heating (magnetic energy) and the pressure. Based on Equation (7), the correlation can be read as:

$$\frac{Q_{\rm vis,1}^{+}}{Q_{\rm vis,0}^{+}} \simeq 4\frac{T_1}{T_0}. \tag{21}$$

Owning to the same reason, there should be a correlation between viscous heating and magnetic energy, i.e., $Q_{\rm vis,1}^{+}/Q_{\rm vis,0}^{+} \simeq E_{B,1}/E_{B,0}$. With Equation (16), the above equation can be modified as

$$\frac{E_{B,1}}{E_{B,0}} \simeq \frac{1}{A_{\rm rad}} \frac{E_{\rm rad,1}}{E_{\rm rad,0}}. \tag{22}$$

As shown in Figure 1, there exists $A_{\rm rad} = 1.8$ for $\beta = 0.1$, so we have the relationship:

$$E_B \propto E_{\rm rad}^{0.55}, \tag{23}$$

which is close to the correlation found in simulations, e.g., $E_B \propto E_{\rm rad}^{0.71}$ (Hirose et al. 2009b). The difference in the index may be related to the following two reasons: (1) the analysis

is quite simple, particularly in dealing with the vertical radiative cooling; (2) the feedback from pressure to stress makes significant contribution.

It is worthy to note that Hirose et al. (2009b) also provided an explanation for the correlation with a toy model based on the energy equation. By using the correlation between $t_{\rm th}$ and $E_{\rm rad}$ ($t_{\rm th} \propto E_{\rm rad}^{s}$) obtained in simulations, they derived the correlation between E_B and $E_{\rm rad}$ ($E_B \propto E_{\rm rad}^{1-s}$). In our analysis, we choose $Q_{\rm rad}^{-}$ to replace their radiative cooling term $E_{\rm rad}/t_{\rm th}$. We will show below that our results are quite similar to theirs.

Equations (3) and (16) can provide the relationship:

$$Q_{\rm rad}^{-} \propto E_{\rm rad}^{1/A_{\rm rad}}. \tag{24}$$

In simulations (Hirose et al. 2009b), the thermal time is calculated by

$$t_{\rm th} = E/Q_{\rm rad}^{-}. \tag{25}$$

With Equations (2), (5), (6) and (24), the above equation can be reduced to

$$t_{\rm th} \propto E_{\rm rad}^{s'}, \tag{26}$$

where

$$s' = \frac{3(1-\beta)(4-3\beta)(\gamma-1)-3\beta(1+\beta)}{(8+\beta)[\beta+3(\gamma-1)(1-\beta)]}. \tag{27}$$

For radiation-pressure-dominated accretion flows, Equation (27) can be simplified as $s' \approx 1-1/A_{\rm rad}$. Thus, Equation (22) indicates the relationship $E_B \propto E_{\rm rad}^{1-s'}$, which is consistent with the correlation in the toy model (Hirose et al. 2009b). Moreover, in the case of $\beta = 0.1$, Equation (27) gives $s' = 0.41$, thus $t_{\rm th} \propto E_{\rm rad}^{0.41}$, which is close to the correlation found in simulations, e.g., $t_{\rm th} \propto E_{\rm rad}^{0.32}$ in simulation 1112a and $t_{\rm th} \propto E_{\rm rad}^{0.44}$ in simulation 1126b of Hirose et al. (2009b).

4. Conclusions and Discussion

In the present work, we have studied the fluctuations of standard thin disks by linear analysis of the time-dependent energy equation together with the vertical hydrostatic equilibrium and the equation of state. Our analytic results show that the delay between magnetic energy and radiation energy is consistent with that in previous simulations. In addition, the analytic power spectrum of radiation energy agrees well with that in simulations. Moreover, the correlation between magnetic energy and radiation energy can be well understood by the analysis, with an index (0.55) being close to that in simulations (0.71).

As indicated by Equation (14), there may exist a break frequency $f_{\rm br} \sim 1/(2\pi A t_{\rm th})$ in $P_{\rm cool}$. The frequency $f_{\rm br}$ may be associated with the high-frequency break observed in the power spectra of luminosity fluctuations (e.g., McHardy 2010), since its value in the inner region of disk is close to that of observed high frequency break. Moreover, the difference between $P_{\rm cool}$ and $P_{\rm vis}$ for $f > f_{\rm br}$, shown by Equation (14), should be taken into account in modeling the high-frequency variability of quasar luminosity (e.g., Mushotzky et al. 2011; Zu et al. 2012). In addition, the similar frequency break may also occur in radiatively inefficient accretion flows, such as advection-dominated accretion flows (Narayan & Yi 1994) and slim disks (Abramowicz et al. 1988).

We thank the referee, Omer Blaes, for helpful suggestions and useful communications to improve the paper. We also thank Feng Yuan and Sheng-Ming Zheng for beneficial discussions. This work was supported by the National Basic Research Program (973 Program) of China under grant 2009CB824800, and the National Natural Science Foundation of China under grants 10833002, 11073015, 11103015, 11222328, and 11233006.

A. The relationship between $P_{\rm vis}$ and P_B

In this Appendix, we try to derive the relationship between $P_{\rm vis}(f)$ and $P_B(f)$ as shown by Equation (17). The evolution of magnetic energy $E_B(t)$ can be simply described as

$$\frac{\partial E_B(t)}{\partial t} = G_B(t) - D_B(t), \tag{A1}$$

where $G_B(t)$ and $D_B(t)$ are respectively the generation and dissipation rate of magnetic energy. With small amplitude perturbations in Equation (A1), we have

$$i\omega t_{\rm dis}\left(\frac{E_{B,1}}{E_{B,0}}\right)_\omega = \left(\frac{G_{B,1}}{G_{B,0}}\right)_\omega - \left(\frac{D_{B,1}}{D_{B,0}}\right)_\omega, \tag{A2}$$

or

$$(\omega t_{\rm dis})^2 P_B(\omega) = P_G(\omega) + P_D(\omega) - \left(\frac{G_{B,1}}{G_{B,0}}\right)_\omega \times \left[\left(\frac{D_{B,1}}{D_{B,0}}\right)_\omega\right]^* - \left[\left(\frac{G_{B,1}}{G_{B,0}}\right)_\omega\right]^* \times \left(\frac{D_{B,1}}{D_{B,0}}\right)_\omega, \tag{A3}$$

where $D_{B,0} = G_{B,0}$, $t_{\rm dis} = E_{B,0}/D_{B,0}$, the symbol "$*$" represents the complex conjugate number, the power spectrum of G_B and D_B are

$$P_G(\omega) = \left|\left(\frac{G_{B,1}}{G_{B,0}}\right)_\omega\right|^2, \quad P_D(\omega) = \left|\left(\frac{D_{B,1}}{D_{B,0}}\right)_\omega\right|^2.$$

Magnetic fields in the accretion disk present exponential growth owing to the magnetorotational instability (MRI, Balbus & Hawley 1991), followed by the dissipation due to some destructive mechanisms. Since the rise and decay phases of channel modes are similar (e.g., Figure 4 of Simon et al. 2009), it is plausible to believe that P_G and P_D is comparable for $\omega \lesssim \pi/t_{\rm dis}$. With the consideration of the delay ($\sim t_{\rm dis}$) between G_B and D_B, the relationship between G_B and D_B can be modeled as

$$\left(\frac{D_{B,1}}{D_{B,0}}\right)_\omega \sim \left(\frac{G_{B,1}}{G_{B,0}}\right)_\omega \exp\left(-i\omega t_{\rm dis}\right). \tag{A4}$$

Substituting this relationship into Equation (A3), we obtain

$$P_D(\omega) = \frac{\left(\omega t_{\rm dis}\right)^2}{2\left(1-\cos\omega t_{\rm dis}\right)} P_B(\omega) \approx \left[\frac{\left(\omega t_{\rm dis}\right)^2}{2} + 1\right] P_B(f). \tag{A5}$$

The above relationship is applicable for $\omega \lesssim \pi/t_{\rm dis}$.

The fluctuations with $\omega > \pi/t_{\rm dis}$ in G_B and those in D_B is unclear, and thus it remains uncertain for $P_G(\omega)$ and $P_D(\omega)$. However, it may be plausible to believe that G_B and D_B are decoupled with each other for $\omega > \pi/t_{\rm dis}$. If we further assume that $P_G(\omega) \sim P_D(\omega)$, Equation (A3) can be reduced to

$$P_D(\omega) \sim \frac{\left(\omega t_{\rm dis}\right)^2}{2} P_B(\omega). \tag{A6}$$

We use this equation to describe the relationship of $P_D(\omega)$ and $P_B(\omega)$ for $\omega > \pi/t_{\rm dis}$. Based on Equations (A5) and (A6), a general form of relationship between P_D and P_B may be simply described as

$$P_D(f) \approx \left[\left(\sqrt{2}\pi f t_{\rm dis}\right)^2 + 1\right] P_B(f). \tag{A7}$$

Since the turbulent kinetic energy follows the fluctuating magnetic energy (Hirose et al. 2009b) and magnetic dissipation dominates over kinetic dissipation, we obtain

$$P_{\rm vis}(f) \approx P_D(f) \approx \left[\left(\sqrt{2}\pi f t_{\rm dis}\right)^2 + 1\right] P_B(f), \tag{A8}$$

which is the exact form of Equation (17). It should be noted that the relationship between $P_{\rm vis}$ and P_B in the short time-scale range ($\omega > \pi/t_{\rm dis}$) is tentatively used in the present work.

REFERENCES

Abramowicz, M. A., Czerny, B., Lasota, J. P., & Szuszkiewicz, E. 1988, ApJ, 332, 646

Balbus, S. A., & Hawley, J. F. 1991, ApJ, 376, 214

Ciesielski, A., Wielgus, M., Kluźniak, W., et al. 2012, A&A, 538, A148

Hawley, J. F., & Krolik, J. H. 2001, ApJ, 548, 348

Hirose, S., Blaes, O., & Krolik, J. H. 2009a, ApJ, 704, 781

Hirose, S., Krolik, J. H., & Blaes, O. 2009b, ApJ, 691, 16

Hirose, S., Krolik, J. H., & Stone, J. M. 2006, ApJ, 640, 901

Kato, S., Fukue J., & Mineshige, S. 2008, Black-Hole Accretion Disks: Toward a New Paradigm (Kyoto: Kyoto Univ. Press)

King, A. R., Pringle, J. E., West, R. G., & Livio, M. 2004, MNRAS, 348, 111

Krolik, J. H., Hirose, S., & Blaes, O. 2007, ApJ, 664, 1045

Lightman, A. P., & Eardley, D. M. 1974, ApJ, 187, L1

Lin, D.-B., Gu, W.-M., & Lu, J.-F. 2011, MNRAS, 415, 2319

Lyubarskii, Y. E. 1997, MNRAS, 292, 679

McHardy, I. 2010, in The Jet Paradigm, ed. T. Belloni (Lecture Notes in Physics, Vol. 794; Berlin: Springer), 203

Mushotzky, R. F., Edelson, R., Baumgartner, W., & Gandhi, P. 2011, ApJ, 743, L12

Narayan, R., & Yi, I. 1994, ApJ, 428, L13

Noble, S. C., & Krolik, J. H. 2009, ApJ, 703, 964

Shakura, N. I., & Sunyaev, R. A. 1973, A&A, 24, 337

Shakura, N. I., & Sunyaev, R. A. 1976, MNRAS, 175, 613

Simon, J. B., Hawley, J. F., & Beckwith, K. 2009, ApJ, 690, 974

Zu, Y., Kochanek, C. S., Kozłowski, S., & Udalski, A. 2012, arXiv:1202.3783

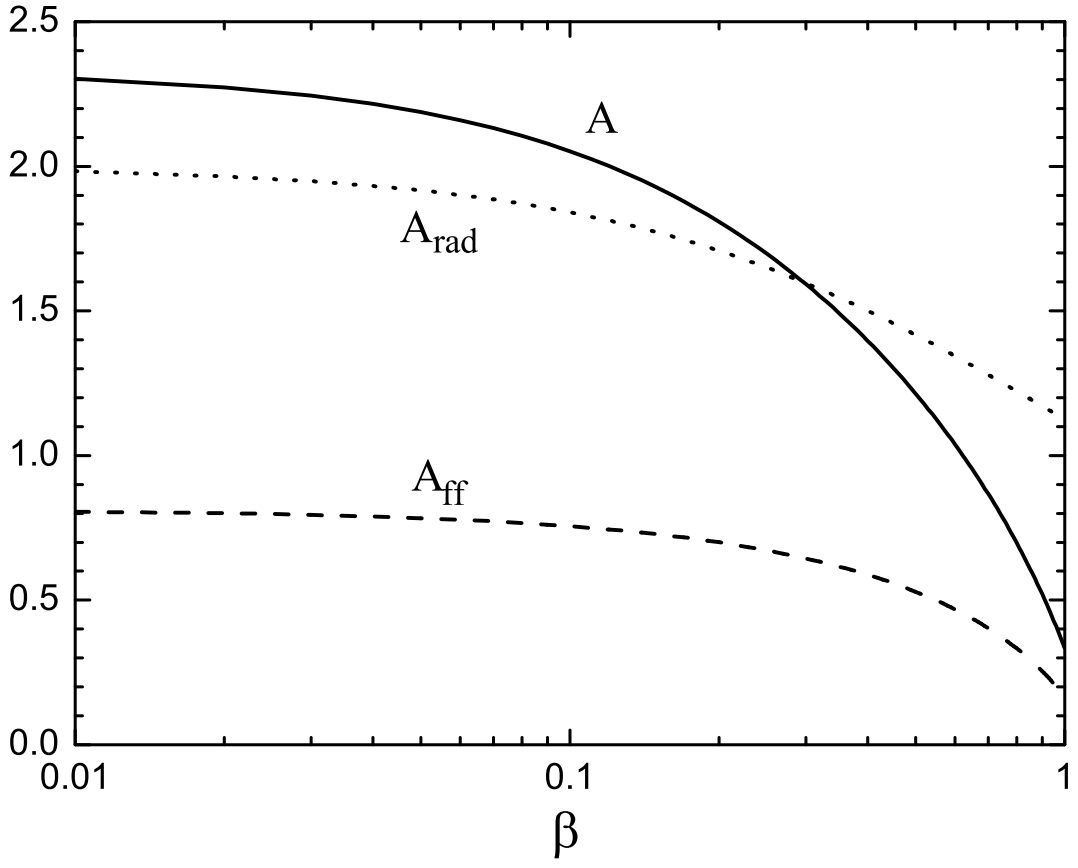

Fig. 1.— Variations of A (solid line), $A_{\rm rad}$ (dotted line), and $A_{\rm ff}$ (dashed line) with β.

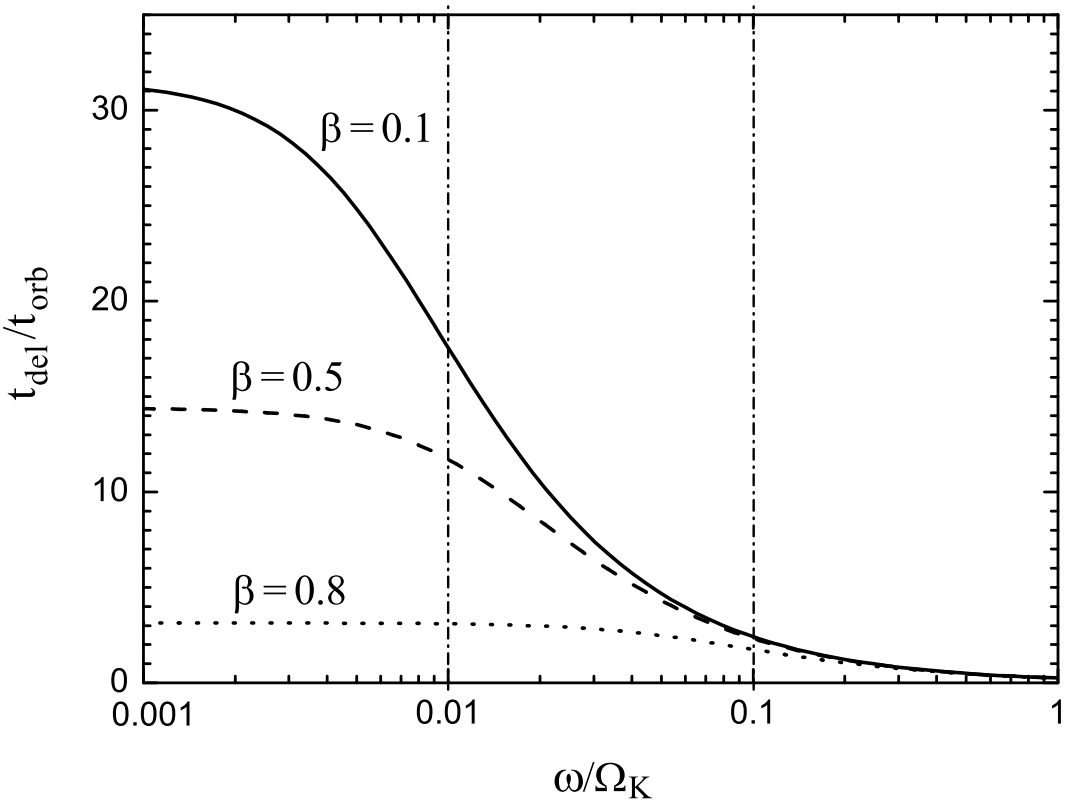

Fig. 2.— The analytic delay of radiation energy compared with magnetic energy for $\beta = 0.1$ (solid line), 0.5 (dashed line), and 0.8 (dotted line). The vertical dot-dashed lines represent two specific frequencies $\omega/\Omega_{\rm K} = 0.01$ and 0.1.

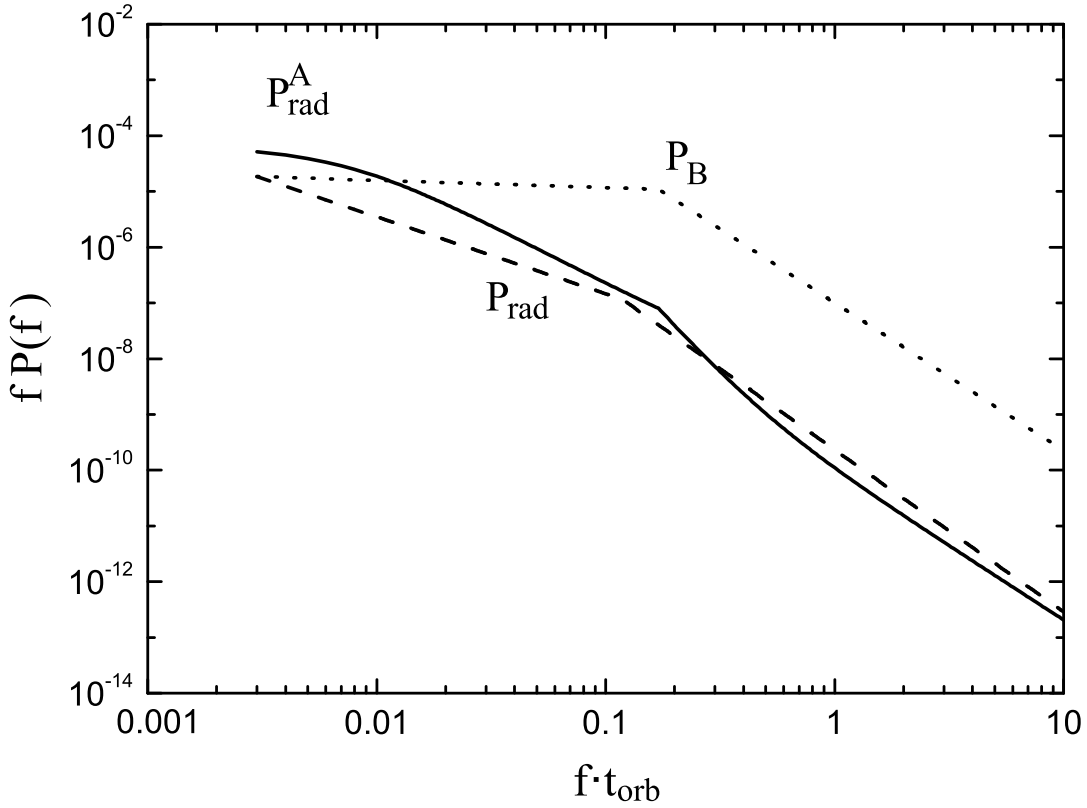

Fig. 3.— A comparison of $P^{\rm A}_{\rm rad}$ (solid line) and $P_{\rm rad}$ (dashed line), where $P^{\rm A}_{\rm rad}$ is calculated with P_B (dotted line).